In vivo sensing to monitor tomato plants in field conditions and optimize crop water management

Filippo Vurro[1] · Riccardo Manfredi[1] · Manuele Bettelli[1,2] · Gionata Bocci[3] · Alberto Luigi Cologni[3] · Sandro Cornali[4] · Roberto Reggiani[4] · Edoardo Marchetti[1] · Nicola Coppedè[1] · Stefano Caselli[2] · Andrea Zappettini[1] · Michela Janni[1,5]

Abstract

Irrigation is key to increasing crop yield and meeting the global demand for food. This study reports the assessment of tomato water consumption by bioristor, a new in vivo an Organic ElectroChemical Transistor-based biosensor. Bioristor enables direct, real-time acquisition of biophysical information about the plant's water requirements directly from the plant sap, and thus the water input can be adjusted accordingly.

The aim of this study is to demonstrate the efficacy of bioristor in rapidly detecting changes in the plant's water status enhancing water use and irrigation efficiency in tomato cultivation with significant savings in the water supply. To this end, experiments were carried out in 2018 and 2020 in Parma (Italy) in tomato fields under different water regimes. The sensor response index (R) produced by bioristor recorded the real time plant health status, highlighting an excess in the water supplied as well as the occurrence of drought stress during the growing season. In both years, bioristor showed that the amount of water supplied could have been reduced by 36% or more. Bioristor also measured the timing and duration of leaf wetting: 438 h and 409 h in 2018 and 2020, respectively. These results open up new perspectives in irrigation efficiency and in more sustainable approaches to pesticide application procedures.

Filippo Vurro and Riccardo Manfredi have contributed equally to this work.

✉ Michela Janni
michela.janni@imem.cnr.it

[1] IMEM-CNR, Parco Area delle Scienze, 37/A, 43124 Parma, Italy

[2] CIDEA-UNIPR – Centre for Energy and Environment, University of Parma, Parco Area delle Scienze, 42, Podere Campagna, 43124 Parma, Italy

[3] Yaxe srl, Via San Martino, 12, 20122 Milan, Italy

[4] Azienda Agraria Sperimentale Stuard scrl, Str. Madonna dell'Aiuto, 7/a, 43126 Parma, Italy

[5] IBBR-CNR, Via Amendola, 165/A, 70126 Bari, Italy

Introduction

Agriculture must provide food for the 10 billion people expected to inhabit the planet by 2050, despite the decreased availability of land and water and the competition from other uses, such as non-food crops, urbanization, or industrial development (FAO, 2021). To date, around 70% of the freshwater available on the planet goes into irrigation (FAO, 2021), yet only a fraction of this is used by crops; the rest is lost via evaporation or consumed by competing weeds.

Crop yields are greatly affected by temperature and rainfall, to the point that water shortage represents the most important environmental factor limiting crop growth, development, and yield (Ben Mariem et al., 2021; Polinova et al., 2019; Wing et al., 2021). Optimization of water use efficiency is key to addressing climate change and food security. Tomato (*Solanum lycopersicum* L.), a high-value crop for the Italian market, is mainly cultivated under irrigation (Corbari et al., 2021), and a non-controlled reduction in water availability could lead to yield losses of up to 50% (Cantore et al., 2016; Takács et al., 2020).

To improve crop yields and optimize farm management, precision agriculture and assist management decisions can concretely enhance sustainability in agriculture. Sensors allow farmers to map the topography and resources in detail (water, nutrient availability, soil topology), as well as variables such as soil pH and temperature (Yin et al., 2021). Several technologies, mainly based on proximal and remote sensing approaches, are currently used to develop, and test multiple indices and techniques for precision water management. Vegetation indices such as the Normalized Difference Vegetation Index (NDVI, Wong et al., 2022) and precision agriculture tools such as unmanned aerial vehicles, are currently being used to develop decision support systems to achieve optimized resource inputs (Loures et al., 2020, p. 202).

The need to establish the plant water content has prompted the development of several approaches to detect the physiological status of the plant and of the surrounding environment (Shafi et al., 2019). These approaches are based on terahertz radiation combined with psychrometry to determine the leaf pressure-volume (Browne et al., 2020; Li et al., 2020). Such approaches entail using VIR/NIR spectroscopy (Jiang, 2020; Zhang et al., 2012); electrical impedance spectroscopy (Ben Hamed et al., 2016; Jamaludin et al., 2015; Janni et al., 2021; Jócsák et al., 2019); infrared technology (Kaiser et al., 2022; Parihar et al., 2021); ultrasonic techniques (Fariñas et al., 2022; Sancho-Knapik et al., 2013); and leaf patch clamps (Cabrita, 2022; Ehrenberger et al., 2012). In addition, soil moisture sensors and electrical conductivity sensors are used to monitor soil temperature and structures (Bonfante, 2019; Polinova et al., 2019), salinity and conductivity, air temperature and humidity, air pressure and wind speed (Shafi et al., 2019). However, these technologies have three main limitations: (i) lack of dynamic and continuous monitoring, (ii) indirect acquisition of the plant water status, and (iii) need for time-consuming data processing.

Bioelectronics is emerging as a powerful approach to monitor plant morphological traits and physiological processes as well as plant-environment interactions. It has been used to monitor or stimulate biological processes (Coppedè et al., 2017; Diacci et al., 2021) and has proved successful in plant sensing and actuation (Bernacka-Wojcik et al., 2019; Diacci et al., 2021; Poxson et al., 2017; Stavrinidou, 2022; Stavrinidou et al., 2015, 2017). An implantable organic electronics ion pump for in vivo delivery of abscisic acid has also been proposed (Bernacka-Wojcik et al. 2019). Several examples of exploiting bioelectronics in precision agriculture, in particular organic electronics (Gebbers & Adamchuk, 2010; Kim & Lee, 2022), have been reported in Dufil et al. (2022) and in Kim and Lee (2022). In

recent years, an in vivo Organic ElectroChemical Transistor (OECT)-based sensor, namely "bioristor" was developed and applied as biosensor for agricultural applications (Coppedè et al., 2017). The sensor can detect the changes in the composition of the plant sap in growing tomato plants (*Solanum lycopersicum*), in vivo and in real time, without interfering with plant functions. Previous work demonstrated its ability to operate directly within the plant stem, thereby enabling in vivo observations of a plant's physiological mechanisms related to ion movements and compartmentalization, under normal as well as stress conditions such as drought (Janni et al., 2019) and salt stress (Janni et al., 2021), or under environmental variations such as vapor pressure deficit (Amato et al., 2021; Vurro et al., 2019) and increase in relative air humidity RH.

The aim of this study is to demonstrate how a bioristor in open field conditions can detect changes in plant water status, thereby enhancing water use and irrigation efficiency in tomato cultivation with significant savings in the water supply.

The novelty of this study lies in the application of bioristor for tomato field monitoring, demonstrating concretely the potential water saving achievable through bioristor supporting its use in pathogen detection and pests' management. Results are discussed in terms of sensor operability and bioristor index acquisition.

Materials and methods

Plant growth and field conditions

Heinz 340 tomato plants were grown up to 2nd stage flowering in two seasons, 2018 and 2020, in two locations in the Parma area of northern Italy, and monitored with bioristors. The climate of both experimental areas is classified according to the Koppen–Geiger classification as Cfb (https://doi.org/10.5194/hess-11-1633-2007).

The two trial seasons were comparable, but not identical, in terms of number of deployed sensors, days of monitoring, and adopted control units. The differences were due to constraints in the plots available and in the overall setup. The bioristor control units used in the second trial had also been improved to make them more suitable to operate in the open field and less dependent upon laboratory instrumentation. In addition, variability between seasons and sites in terms of weather, soil, and experimental setup is clearly unavoidable during field validation of sensors in open field conditions.

In 2018, the experiment was carried out in Azienda Stuard, Parma (60 m a.s.l., 44° 48′ 29.888″ N 10° 16′ 29.074″ E) in collaboration with Mutti SpA (https://mutti-parma.com/). Three experimental plots, consisting of three rows for each irrigation regime, were monitored (Fig. 1A). To avoid any water leakage compromising the validity of the measurements, only the middle row of each plot was used for bioristor measurements. Ten plants for each irrigation condition, distributed across an area of about 50 m^2, were equipped and monitored continuously with a bioristor for 62 days, from flowering to harvest. Three irrigation regimes were applied. The control was set as 100% in line with recommendations by the regional irrigation advisory service Irriframe. It evaluates weather, soil and groundwater data obtained from farmers and from regional agencies and provides crop-specific irrigation regimes (https://www.irriframe.it/Irriframe). Two regimes were set to receive 80% and 60% of the full irrigated plot (100%). In the 2018 experiment, differential irrigation started eight days after the bioristor installation, while in 2020, the experiment
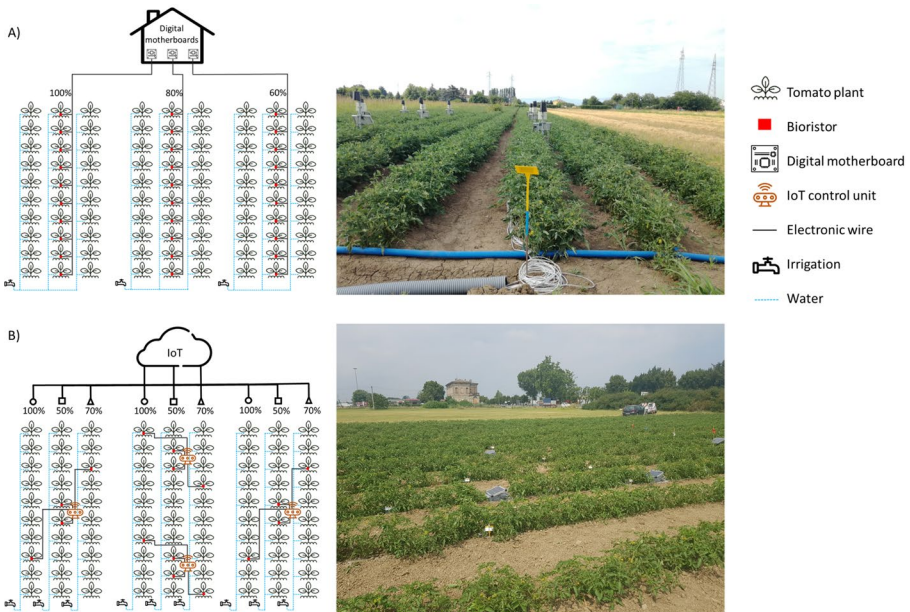
Fig. 1 Sketch and real-field image of the field trial. **A** 2018, **B** 2020

was performed in collaboration with Yaxe Srl for 54 days in a commercial tomato field in Parma (44° 49′ 02.4″ N 10° 14′ 37.5″ E).

Based on the results obtained in 2018, the irrigation was set at full water regime (100%, as in Irriframe recommendations), and 70 and 50% of the fully irrigated plot (Fig. 1B). One bioristor was installed in four plants for the 100% regime, four plants for the 70 and 50% regimes. The plants were monitored in total for 54 days. In the 2020 experiment, due to a delay in the implementation of the irrigation system, differential irrigation started after 21 days.

A drip watering system was used for irrigation in both years, where the regimes were differentiated according to the time of water flow. All plots were regularly irrigated according to 100% of Irriframe advice prior to the start of the differential irrigation. The full list of phytosanitary treatments and operations is reported in Suppl. Table 1.

In both years, in all plots subjected to multiple water regimes the bioristor's response (R) was compared to identify differences between the different irrigation regimes in terms of bioristor output. The effects of the treatments on the bioristor response were then analyzed to further understand the bioristor's ability to monitor plant eco-physiology.

The bioristor sensors, principles and preparation

The bioristor is an OECT-based biosensor made up of two functionalized textile fibers (polypropylene) serving as the channel and the gate of a transistor.

The bioristor is directly inserted into the plant stem (Janni et al., 2019), and it measures the changes in ion concentration in the plant sap which is continuously read via an IoT system (Finco et al., 2022). The working principle is based on doping-state changes in the

semiconductor channel material due to electrolyte-ion injections which modify the electrical conductivity (Marquez et al., 2020; Tarabella et al., 2012). A positive input voltage at the gate electrode modulates the channel current by pushing cations from the electrolyte into the PEDOT:PSS matrix, thus modifying channel conductivity (Friedlein et al., 2018; Janni et al., 2021).

The sensor's response is the result of the relationship between the sensor and the changes occurring in the plant sap composition and ion concentration during growth, development and under abiotic stress. Under drought stress, the sensor response drops significantly because of the diminished ion concentration in the plant sap derived from low plant transpiration and root water absorption (Janni et al., 2019). A significant increase in the R was observed (Amato et al., 2021; Vurro et al., 2019) in high relative humidity conditions (RH) and low vapor pressure deficit (VPD).

Bioristor preparation

Prior to functionalization, each thread was cleaned with a plasma oxygen cleaner (Femto, Diener electronic, Ebhausen/Germany) to improve the thread's wettability and facilitate the adhesion of the aqueous conductive polymer solution. This step enhances the performance of the sensors by removing any impurities or contaminants on the fibers, and increases the surface area for the polymer adhesion. An aqueous solution containing PEDOT:PSS (Clevios PH1000, Starck GmbH, Munich, Germany) and dodecyl benzene sulfonic acid (2% v/v) was prepared and stirred for five minutes to ensure homogeneity.

The solution obtained was deposited onto polypropylene fibers using a drop-casting technique in an amount of 50 μL/cm. This resulted in the formation of a thread with a cross-sectional area of 1.42 mm × 0.25 mm. This approach means that the thickness and shape of the sensor can be controlled precisely, polypropylene fibers can be used as a substrate which offers biocompatibility and mechanical stability, and the fibers can be infused with the conductive polymer, which is essential for the sensors to function effectively.

The entire process is repeated three times to complete the preparation of the sensors. Next, the fibers were treated with highly concentrated sulfuric acid (95%) for 20 min. This improves the crystallinity, electrical properties, and durability of the polymer by replacing the use of ethylene glycol (10% v/v) treatments to improve the electrical conductivity and long-term stability of the polymer. Finally, the fibers were washed with water, and subjected to annealing for 1 h at 130 °C (Coppedè et al., 2017).

The bioristor is covered by patents in Europe (IT201600130803A1) and the USA (Pat. n. WO2018116149A1).

Bioristor integration in plants and signal acquisition

After functionalization, 2 cm of the prepared fibers were inserted into the plant stem, with a distance between the two threads of 5 mm in tomato plants at 15 days after transplant (5–6 leaves) at 10 cm above the soil surface (Janni et al., 2019) (Fig. 2A and B). The channel is connected by bonding two thin electrical wires to both sides, while the gate is connected only on one side to the electrical wire. These wires are fixed on a 3D printed holder made of blue polymeric material, to improve bioristor stability (Fig. 2A) and connected by wires to the digital motherboard (Fig. 3A) or to the control unit (Fig. 3B, C).

A constant voltage ($V_{ds} = -0.1$ V) was applied between the source and drain terminals of the channel, resulting in a continuous current flow, and a positive voltage at the gate
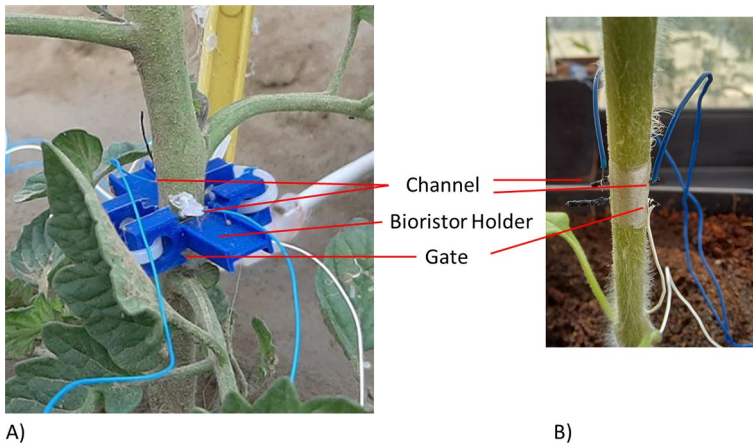
Fig. 2 Bioristor implementation in plants. **A** Example of bioristor inserted into tomato plants in open field. The bioristor is composed of a channel and a gate connected to electrical wires in its current version. A holder ensures that no damage is caused to the plant stem due to the weight of the wires; **B** the channel and gate connected with wires without the holder
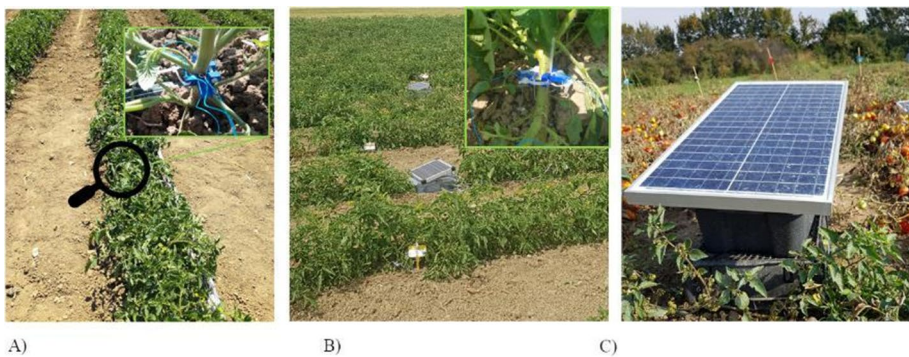

Fig. 3 **A** 2020 Bioristor application. **B** 2020 Field, **C** 2020 bioristor control unit

($V_g = 0.6$ and 1 V in 2018; $V_g = 0.5$ V in 2020) was applied thus leading to a decrease in the channel conductivity due to the cations pushed from the electrolyte into the channel. The current (I_{ds}) was monitored continuously.

The sensor response (R) is the main index acquired and is proportional to the sap cation concentration. It is given by the expression:

$$R = \frac{|I_{ds} - I_{ds0}|}{I_{ds0}},$$
(1)

where I_{ds0} represents the current across the channel when $V_g = 0$. The sensor response R was recorded for the entire productive cycle.

The I_{gs} was also monitored and is the current flowing through the solution from the gate to channel when a positive gate bias is applied. The difference $\Delta I_{gs} = I_{gs} - I_{gs0}$ is related to

the sensor wetting status, where I_{gs0} is the current across the solution when $V_g = 0$ (Gentile et al., 2020).

The acquisition of the sensor response R is based on the relative change in the channel current. No calibration is required. The current flowing through the channel when the gate is off (I_{ds0}) is used to calculate the R at each time point continuously.

Two time constants τ and τ_{gs} of the sensor were also evaluated in a multivariate analysis. τ and τ_{gs}, computed by fitting the non-linear drain and gate current curves, are related to the time that ions take to enter the polymer, τ, and the ions diffusivity in the solution, τ_{gs}, respectively (Coppedè et al., 2014, 2017; Vurro et al., 2019). The first derivatives as a function of time of R, ΔI_{gs}, τ, and τ_{gs} parameters (dR, dΔI_{gs}, dτ, and dτ_{gs}) were also calculated to highlight specific trends (Vurro et al., 2019).

R is the result of the relationship between the sensor and the changes in the plant sap composition and ion concentration during growth, development and under abiotic stress. Under drought, R drops significantly because of the reduced ion concentration in the plant sap due to the low plant transpiration and root water absorption (Janni et al., 2019). Moreover, in high relative humidity conditions and low vapor pressure deficit (VPD), a significant increase in R was observed (Amato et al., 2021; Vurro et al., 2019). Rainy events increase the air relative humidity (RH%) and decrease the VPD and a rapid increase in the R was observed.

Based on these considerations, to demonstrate the reproducibility of the sensor's response, an in vitro experiment was performed. The results of the sensor response of seven replicates of bioristor, in the range 10^{-4}–10^{-2} M NaCl solution, were reported (Suppl. Table 2).

Bioristor IoT control unit

The bioristor control unit was optimized across the two field trials to improve its performance and enable the use of the device in open fields.

In the 2018 setup, each bioristor sensor was connected to a digital acquisition board NI USB-6343 multifunction I/O device (National Instruments, Austin, TX, USA) through electrical wires. It is a multi-channel analog-to-digital converter connected to a PC, where the readout data is processed using custom and then saved in the cloud. The sensor currents were converted to voltage, which is more easily readable by the NI board, through a resistor. The board is equipped with a 16 bit ADC (5 V full-scale), and currents are read through a 10 Ohm resistor. The current resolution is about 8 µA. The data from each connected bioristor was acquired every second, locally saved on the PC, and then sent to the cloud.

In the revised 2020 setup, the IoT control unit was based on the Arduino DUE system and connected to a 12 V 12 Ah lead battery powered by a 10 W photovoltaic panel. Bioristor data was locally saved on a micro-SD memory card and transferred to the cloud via a 4G connection. This setup allowed for the maximization of the signal to noise ratio using customized electronic circuits to amplify the bioristor signals, as well as local analysis of the raw data.

Signals were read through an amplification system that gave a more accurate measurement of the currents. The sampling rate was 1 Hz, and each control unit was able to read up to four sensors. The control unit has a 12 bit ADC (5 V full-scale); the maximum current full-scale is 7 mA, the current resolution is about 1.5 µA. A micro-weather unit was

also incorporated into the control unit (DHT11 module, Seeed Technology Inc., Shenzhen, China) to monitor air temperature (T°C) and relative humidity (RH).

In both experiments, the gate was turned ON (V_g = 0.6 V in 2018 season; V_g = 0.5 V in 2020 season) for 15 min and OFF (0 V) for 15 min. At every gate that was switched on, R was calculated every 15 min considering the last two values of I_{ds} and I_{ds0}.

Environmental conditions and soil characteristics

In 2018 rain abundance, as well as temperature and relative humidity at 2 m above the ground, were recorded by ARPAE agrometeorological station (https://simc.arpae.it/dext3r/). Soil sensors from Agricultural support (http://www.agriculturalsupport.it/prodotti-colture-orticole) were also exploited to verify the changes in the soil moisture.

In 2020, the environmental conditions were monitored via Pycno sensors (https://pycno.co/), which monitor soil volumetric water content and temperature at 10, 25, 40 and 55 cm depth, and air temperature, humidity, and solar radiation.

Based on the parameters recorded with the datalogger, the VPD value was calculated as follows (Vurro et al., 2019):

$$VPD = \left(1 - \frac{RH}{100}\right) \times SVP, \tag{2}$$

where RH is relative humidity and SVP is saturated vapour pressure.

The SVP was calculated with the following equation (Murray 1967):

$$SVP = 610.7 \times 10^{\frac{7.5T}{237.3+T}}, \tag{3}$$

where T is the temperature measured in the growth chamber.

Ground physiological measurements

In 2018, to validate bioristor in monitoring plant health and water use efficiency in field, classical physiological measurements were performed. Three plants for each regime were analyzed to calculate the relative water content (RWC) of the leaves (Buffagni et al., 2020).

Leaf RWC (%) was measured in control and stressed leaves. Two leaves were clipped from five plants from each regime and placed in 50 mL tubes. Fresh weight (FW) was immediately recorded, then leaves were soaked in distilled water for 4 h at room temperature under constant light. The turgid leaf disks were then rapidly blotted to remove surface water and weighed to obtain the turgid weight (TW). Leaves were dried in the oven at 80 °C for 24 h to record the dry weight (DW). The RWC was calculated according to the formula (Barrs & Weatherley, 1962):

$$RWC(\%) = \frac{FW\text{-}DW}{TW - DW} \times 100. \tag{4}$$

Chlorophyll content was assessed with a SPAD 502 m (Konica Minolta, Ramsey, USA). Ten measurements for each plant of three expanded leaves were recorded along the leaf length in five plants for each regime. The relative SPAD values were recorded.

The stomatal conductance of the leaves was measured using an SC1 leaf porometer (Decagon Devices, Pullman, WA, USA) to evaluate the transpiration process. Five plants (one leaf for each plant) were recorded from 06:00 am to 08:00 am.

Data analysis and statistics

R data were analyzed with MATLAB (https://uk.mathworks.com/) and Microsoft Excel 2016 to smooth out variations related to the circadian cycle (Coppedè et al., 2017; Janni et al., 2019) by calculating the rolling mean. The aim was to reduce background noise and thus highlight the variations due to drought.

The R data were then subjected to ANOVA using MATLAB (https://uk.mathworks.com/) .In addition, the p-value was calculated and is reported in Suppl. Tables 3 and 4. The standard error was calculated on plant physiological data using Excel 365 ProPlus (Microsoft Corporation, Redmond, WA, United States). Data were analyzed from five plants with one, two and three replicates for stomatal conductance, RWC and SPAD measurements, respectively. The current data from the bioristors were fitted using least square minimization performed with the "fminuit" function in MATLAB.

To evaluate the effect of differential treatment and the contribution of each parameter to the plant health under drought stress, PCA was performed using all the bioristor parameters collected from plants at 30–34 days in 2018 and at 32–39 days in 2020. PCA was performed using the R "prcomp" function and represented as a biplot using the R package "factoextra". The first two principal components PC1 and PC2 and the corresponding component loading vectors were visualized and summarized in a biplot, in which component scores (indicated with dots) were colored in relation to the specific regime (Kassambara & Mundt, 2016).

Results

Bioristor monitoring in multisite experiments

The bioristor transfer characteristics were verified by measuring Ca^{2+}, K^+, and Na^+ in vivo, with reference to concentrations included in the range found in leaves. This demonstrated that a bioristor can detect small changes in the salt-related ion concentrations in the plant sap (Janni et al., 2021).

In 2018, the R index trend showed no significant difference between water regimes for almost the entire season. The first 5–7 days after bioristor integration in plants correspond to the implantation and stabilization phase of the sensor, also previously reported in controlled conditions (three days in pots, Janni et al., 2019). The R observed during the stabilization phase was not used to calculate the theoretical water savings (TWS). In fact, in 2018 several rain events characterized the growing season and substantially nullified the effect of differential irrigation for almost the entire duration of the experiment. The difference among the regimes was only observed in the interval between days 28 and 35, when a severe drought occurred (Supplementary Fig. 1, Supplementary Table 3).

A major and rapid peak in the R signal (200–400%) was observed in correspondence with each rain event (days 5–7, 12, 13, 16, 18, 23, 25, 42, 47, 58, 59, Suppl. Figure 1 A) due to the increases in relative humidity (RH%) and, in turn, a decrease in the VPD (Fig. 4 in Vurro et al., 2019).

Fig. 4 R monitored in 2018 for 62 days (100% regime: blue line, 80% regime: dark red line, 60% regime: dark gray line) and vapor pressure deficit (VPD, black line) in the 2018 season. R plots are the average response of 10 plants for each regime (Color figure online)
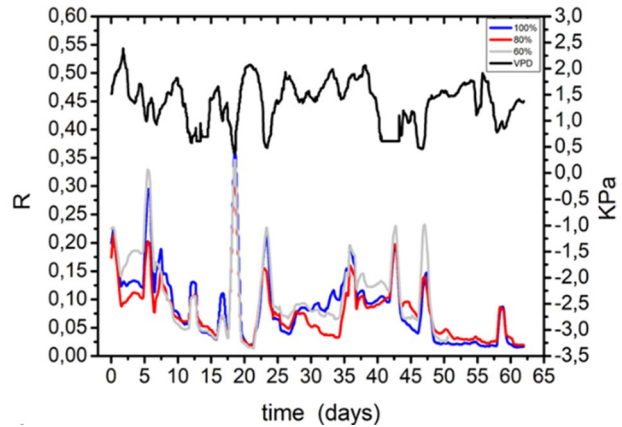
A considerable decrease in the R signal was observed in all plots between days 5 and 20 in relation to the treatment with ACTARA 25WG, which was administered to counteract an aphid infestation. In fact, a key time window for the entire experiment was observed between days 22 and 44, when the reduction in rain events and the increase in temperature meant that the R index response was different for each regime.

Between days 25 and 35, a significant difference in R was observed among the regimes ($p \leq 0.05$, Supplementary Table 3).

The sensor response drops significantly under drought due to the block of transpiration which then leads to a reduction in the ion concentration in the xylem sap and their redistribution to maintain the plant osmoregularity (Janni et al., 2019).

From days 31 to 35, the R of the 80% regime showed a 40–60% decrease in the sensor response compared with the 100% regime, and a 10–40% reduction in the R of the 60% regime was also observed. Data suggest the occurrence of more severe drought stress in the 80% regime compared to the 60% regime, in accordance with measurements recorded by the soil sensors (Fig. 4).

Between days 40 and 62, there was a gradual decrease in R in all the regimes, except for days 42, 47, 58 and 59 when heavy rains occurred and the R trend rapidly increased as expected. In fact, fruit ripening causes leaf senescence and a reduction in transpiration (Mundim & Pringle, 2018). This leads to a subsequent decrease in the concentration of ions in the plant sap, which explains the decrease in the R signal observed (Fig. 4).

The 2018 field pilot allowed to successfully validate the efficacy of the bioristor to detect physiological changes in plants as confirmed by the physiological data collected. The stomatal conductance trend showed a significant reduction in the transpiration process between regimes starting from day 22 up to day 27 (Fig. 5A), whereas neither the RWC nor the SPAD values showed a significant difference between regimes. This, confirms the high sensitivity of the bioristor's index in the early detection of drought stress (Fig. 5B, C, Janni et al., 2019).

The PCA performed on bioristor data showed that the first two principal components (PC1 and PC2) explained 72.4% of the total variance and highlighted a clear division of variables into three different groups along the first component (PC1), thereby confirming that the effects of drought stress on plant physiology are correctly tracked by the sensor (Fig. 6). The first PC (PC1) alone explains 47.3% of the phenotypic variation with controls and drought-stressed plants well separated in the biplot, thus indicating the efficacy of
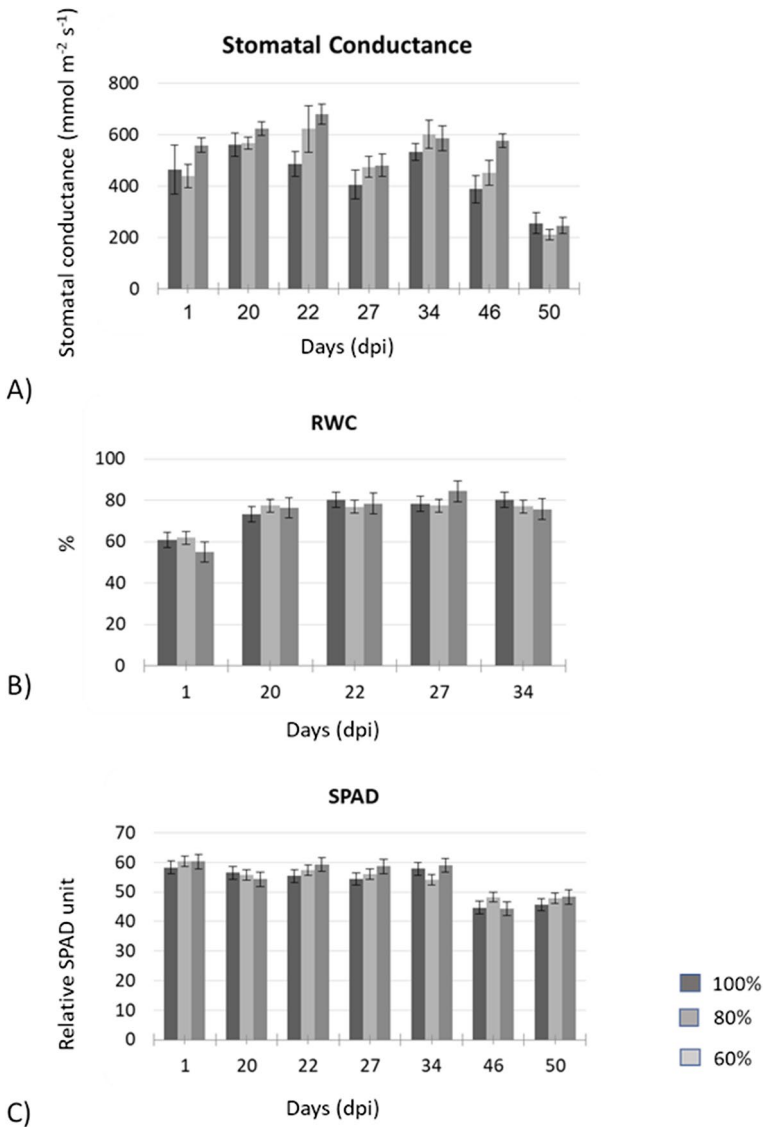
Fig. 5 Physiological analyses performed in real time (dpi = days post insertion) in 2018. **A** Stomatal conductance, **B** relative water content (RWC), **C** chlorophyll fluorescence expressed as relative SPAD units. Error bars represent standard error

the various irrigation regimes. The sensor response R, ΔI_{gs} and their first derivative (dR, dΔI_{gs}) are negatively correlated with τ_{gs} and τ.

In 2020, the R index trend was comparable for all plots, as expected, which were irrigated regularly up to day 21 (Fig. 7). The deviation in the R response of the 50% regime from day 7 to day 15 is discussed in the next section. Starting from day 21, irrigation was managed differently for each regime and a significant difference in the R signal was observed (Supplementary Table 4). A severe drought stress was detected in the 50%
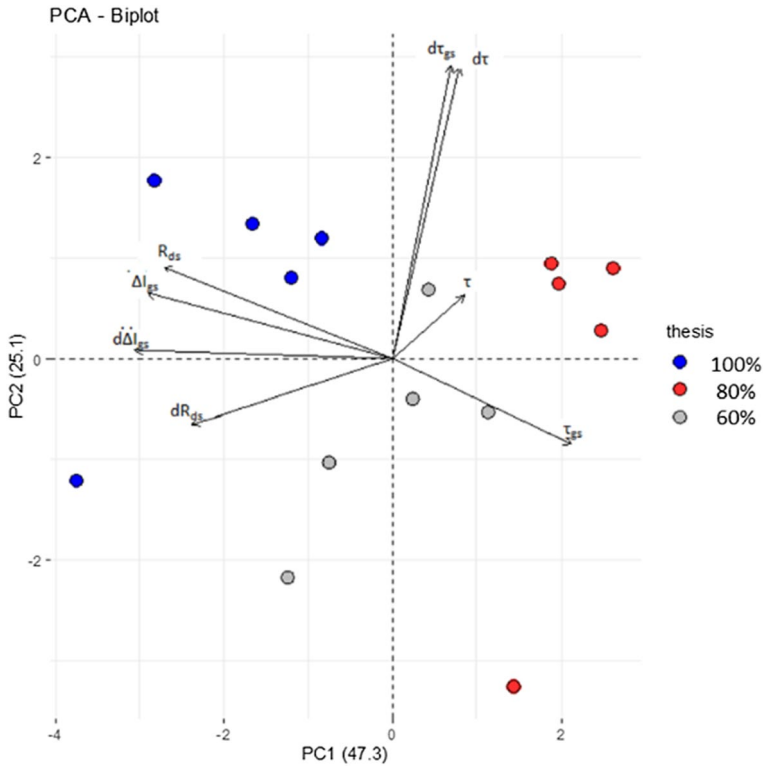
Fig. 6 PCA of the parameters acquired via bioristor in the 2018 trial. The component scores (shown in points) are colored according to the regime (blue 100%; red 80%; gray 60%). The component loading vectors (represented in lines) were superimposed proportionally to their contribution. ΔI_{gs}: difference between minimum and maximum gate current values. τ and τ_{gs}: time constants. From the acquired data, the first derivatives of R, ΔI_{gs}, τ and τ_{gs} (dR, dΔI_{gs}, dτ and dτ_{gs}) were calculated. PC1 and PC2 explain 72.4% of the variability observed. Each dot represents the daily mean for each detected stress day (30–34) (Color figure online)

Fig. 7 Plot of R monitored in 2020 for 54 days (100% regime: blue line, 70% regime: red line, 50% regime: gray line) and vapor pressure deficit (VPD, black line) during 2020 trial. R plots are the average response of four plants for each regime (Color figure online)
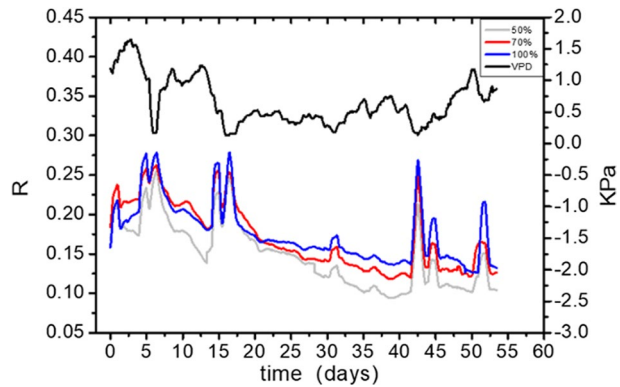
regime (33% R reduction, p-value ≤ 0.05), whilst the 70% regime showed an intermediate decrease (17% R reduction). As observed by other authors, under fruit ripening the R signal declined as an effect of the reduction in transpiration (Mundim & Pringle, 2018).

There was a rapid increase in the R index also due to rain in 2020. The R index varied from 26 to 122% with rain on days 5, 6, 15–18, 32, 37, 38, 43–45, 47, 48 and 52 (Supplementary Fig. 1B). This observation further supports the ability of bioristor to detect leaf wetting due to increased environmental VPD (Fig. 7).

A PCA of the 2020 data confirmed the observations made in the 2018 trial. The first two components (PC1 and PC2) explain 64.2% of the total variance. The variance among the groups is more closely associated with the variance captured by PC2 than by PC1. The three regimes are well separated in the biplot, highlighting how the bioristor can detect physiological changes due to drought stress (Fig. 8). However, the distribution of the groups was not homogenous, as observed in our previous trial in 2018. Specifically, the groups associated with the 100% and 70% regimes form a cluster-like pattern, whilst the scores for the 50% regime were more separated. When all variables
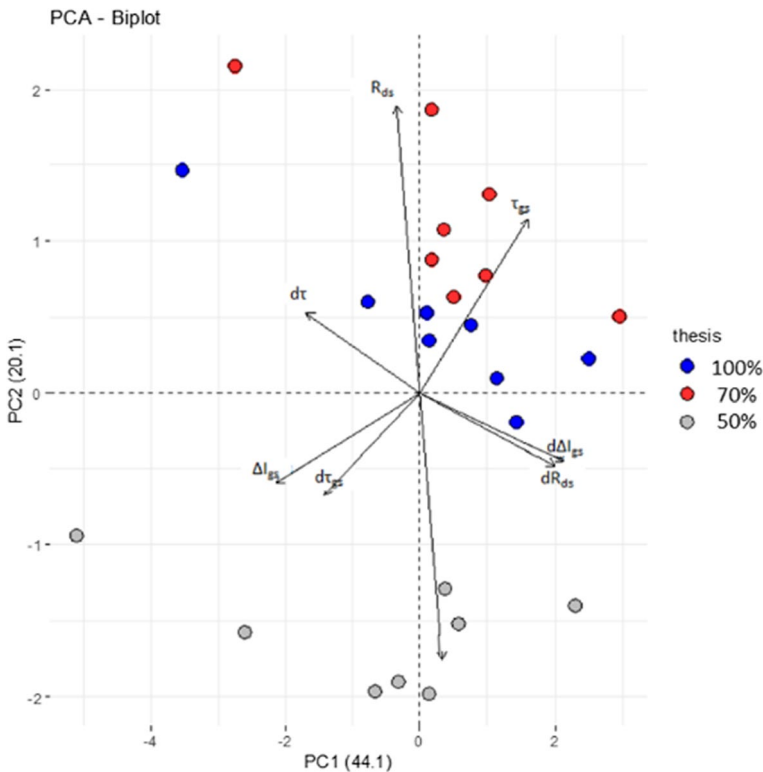

Fig. 8 A PCA of the parameters acquired via bioristor in the 2020 trial. The component scores (shown in points) are colored according to the agronomic groups (blue, 100% regime; red, 70% regime; gray, 50% regime). The component loading vectors (represented in lines) were superimposed proportionally to their contribution: ΔI_{gs}; difference between minimum and maximum current gate values, τ and τgs; time constant. From the acquired data, the first derivative of R, ΔI_{gs}, τ and τ_{gs} (draw, $d\Delta I_{gs}$, $d\tau$ and $d\tau_{gs}$) were calculated. PC1 and PC2 explain 64.2% of the variability observed. Each dot represents the daily mean for the principal detected stress days (32–39)

were considered, the 100% and 70% regimes of the 2020 trial clustered closer than the 100% and 80% regimes of 2018, suggesting that all the bioristor variables should be considered.

The R trend recorded for each plant is highly reproducible (Supplementary Fig. 2). In open field, the sensor response is strongly dependent on the interaction of each plant with the environment. Consequently, the sensor's performance should be considered in terms of the signal trend variation, rather than the R value of an individual plant.

This was confirmed in vitro, where plant physiological and morphological mechanisms have no influence, and the environment has no impact. The sensor response reproducibility was extremely high, calculating the R on seven sensor replicates, in a range of 10^{-4}–10^{-2} M NaCl solution (Supplementary Table 2).

Estimation of potential water saving using the bioristor

The R index was also compared with the tomato yield and quality indices recorded at harvest (Table 1).

In both trials (2018 and 2020), the tomato yield differed only slightly between the regimes. This resulted in a comparable percentage in terms of commercial yield. In 2018, only the 60% regime exhibited a significant reduction in the commercial production due to an increase in rotten fruit, most probably due to the drought suffered during flowering (Millones-Chanamé et al., 2019).

Based on the R index variations recorded during the experiment, in both trials, the theoretical water saving (TWS) was calculated and is reported in Tables 2 and 3. In the 2018 trial, all regimes performed similarly during the entire season. The R index slope was significantly different for few days only (28–35) between the different water regimes ($P \leq 0.05$) and was dependent on the amount of water input. Based on the yield recorded for all regimes, it was assumed that the amount of water provided in the 60% regime would be sufficient to achieve the good final yield expressed in marketable fruit percentage, except for the 28–35 day window, when the full amount of water applied to the 100% regime was required to overcome the severe drought.

For the 2018 trial, the percentage of theoretical water saving reported as achievable using the bioristor signal as a guide for irrigation was computed using the formula:

$$TWS(\%) = \frac{Vt_{100\%} - Vt_{TBI}}{Vt_{100\%}} \times 100, \tag{5}$$

Table 1 Tomato yields in the 2018 and 2020 trials

Season	Regime (%)	Marketable fruit %	Unripe fruit %	Rotten fruit %	Apical rot n°
2018	100	89.6	5.1	5.3	0.0
	80	89.7	5.1	5.1	0.0
	60	87.7	2.5*	9.8*	0.0
2020	100	91.7	6.7	1.6	1.0
	70	75.6	19.8	4.6	5.5
	50	86.3	8.4	5.3	4.0

*Significant different ($P \leq 0.05$)

Table 2 Irrigation volumes and water savings (TWS) calculated based on the response of the bioristor sensor in 2018

Days	100% Irrigation (m³/ha)	80% Irrigation (m³/ha)	60% Irrigation (m³/ha)	Theoretical bioristor irrigation (m³/ha)	Theoretical water saved (%)
8	88.80	71.04	53.28	53.28	40.0
15	111.00	71.04	53.28	53.28	52.0
25	66.60	53.28	39.96	39.96	40.0
26	88.80	71.04	33.30	33.30	62.5
28	66.60	39.96	26.64	66.60	–
30	222.00	177.60	133.20	222.00	–
32	155.40	124.32	93.24	155.40	–
34	199.80	159.84	119.88	119.88	40.0
37	133.20	106.56	79.92	79.92	40.0
39	133.20	106.56	79.92	79.92	40.0
40	133.20	79.92	53.28	53.28	60.0
51	133.20	79.92	53.28	53.28	60.0
54	133.20	79.92	53.28	53.28	60.0

Table 3 Irrigation volumes and water savings (TWS) calculated based on the response of the bioristor sensor in 2020

Days	100% Irrigation (m³/ha)	70% Irrigation (m³/ha)	50% Irrigation (m³/ha)	Theoretical bioristor irrigation (m³/ha)	Theoretical water saved (%)
21	143.27	95.99	75.8	95.99	33.0
23	143.27	95.99	75.8	95.99	33.0
26	143.27	95.99	75.8	95.99	33.0
28	143.27	95.99	75.8	95.99	33.0
30	143.27	95.99	75.8	95.99	33.0
33	143.27	95.99	75.8	95.99	33.0
35	143.27	95.99	75.8	75.8	47.1
37	143.27	95.99	75.8	143.27	–
40	226.2	151.55	57.87	226.2	–
42	226.2	151.55	57.87	57.87	74.4
46	226.2	151.55	57.87	57.87	74.4

where $Vt_{100\%}$ represents the total volume of water used for irrigation (100% control regime), as determined by the Irriframe service (Table 2), and Vt_{TBI} indicates the total volume of water that would have been used if irrigation had been managed with the bioristor, based on the signal recorded for the other regimes (Table 2).

Based on the above formula, if the bioristor had been used in 2018 to guide the irrigation system, the average water saving would have been 36% (Tables 1 and 2).

In the 2020 trial, yield was not in line with irrigation. In fact, the 70% regime showed a significant, larger decrease in yield (marketable fruit) compared with the 50% regime, whereas a smaller decrease in yield was observed in the 50% water regime compared with

the 100% water regime. Based on the bioristor data and yield performance, in 2020 the TWS was 38% (Tables 1 and 3).

Discussion

Water scarcity increasingly threatens food security and nutrition due to the importance of water for food systems, agricultural production, food processing, households, and consumers (FAO, 2021).

Italy is a big water consumer since agriculture is one of the main sources of income. A total of 41.67% of the entire agricultural land in Italy is irrigated. Out of 9 Mha of cultivated land, 4 Mha are equipped for irrigation. A total of 17 billion m^3/year of agricultural water are consumed in Italy alone (Ritchie & Roser, 2020).

Precision agriculture is gaining interest as the related technologies can observe, measure, and apply exact quantities of water to crops on a large scale. Several sensors are extensively used in precision agriculture management. In particular, proximal soil sensors play a critical role in smart and precision agriculture by monitoring real-time physical signals in the soil, such as temperature, moisture, pH, and pollutants, and providing key information to optimize crop growth, fight against biotic and abiotic stresses, and enhance crop yields (Yin et al., 2021). However, proximal sensors only return data related to the plant proximity and do not provide information on what is really occurring in the plant system.

An in vivo sensing approach was used in this study to understand the potential water savings through continuous and real-time monitoring of tomato crops in the open field during the entire growth season.

The output of bioristor sensor is strongly related to the plant's water status and to physiological and phenotypic changes due to drought. The high sensitivity and short time response (within minutes) of the bioristor index R increases the possibility and timeliness for determining a water deficit in a plant at a particular crop stage, thereby improving the efficiency of plant-based irrigation scheduling (Gentile et al., 2020; Gu et al., 2020; Janni et al., 2019; Vurro et al., 2019).

In 2018 and 2020, an excess in irrigation was identified by comparing the final yields with the water used. A minimum reduction of 36% in 2018 and 38% in 2020 in water use would have been achievable if bioristor had been used to guide the irrigation system.

Previous studies have used a life cycle assessment to estimate the amount of water saved for different crops. Fotia et al. (Fotia et al., 2021) demonstrated that precise irrigation by DSS-based management can reduce the overall environmental impact per 1 ton of olives by 5.3–18%, or by 10.4–22.6% per 1 ha of cultivated land. Balafoutis et al. (Balafoutis et al., 2017) reported that variable-rate application of water in a vineyard can reduce greenhouse gas emissions by 8.8%.

In the experiments carried out in two years and in two locations, the bioristor-based approach reported in this study provided additional tools to: (i) save water for irrigation, (ii) decreasing the water input required in tomato crops by 36–38%. Based on the collected data a complete algorithm for a fully operational decision support system based on the in vivo bioristor data, have been developed with the aim of identifying thresholds for the early warning of drought stress (Fig. 9).

A novelty of this work is the possibility to calculate form the R index, the timing and duration of leaf wetting were also measured through the bioristor: 438 h in the 2018 experiment, and 409 h in 2020 (Table 4).
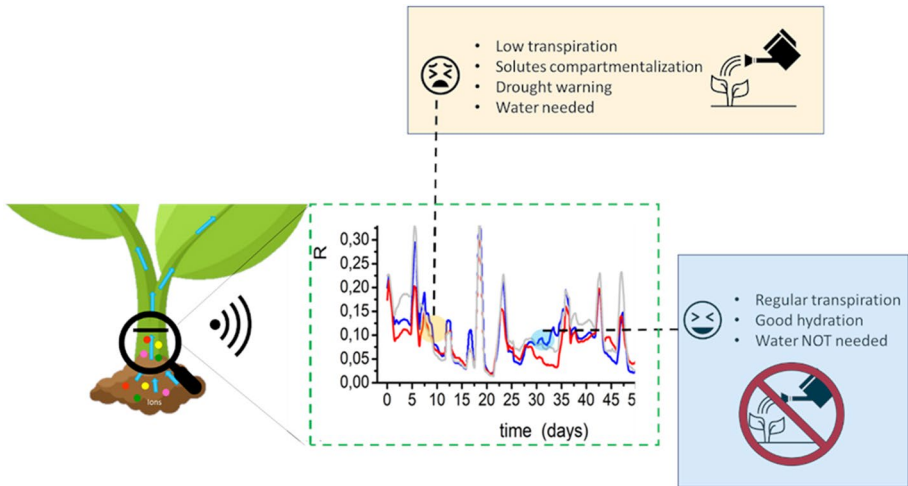
Fig. 9 Bioristor working principle and features. Sensor response and data interpretation in relation to water supply and needs

Table 4 Leaf wetting timing and duration calculated over the whole season in 2018 and 2020

Season	Leaf wetting timing (days)	Leaf wetting duration (h)
2018	18	438
2020	17	409

Leaf wetting plays a major role in plant physiology with direct or indirect effects on plant function. For example, in leaf wetting by dew, the transpiration rate can decrease, thereby mitigating water stress at times of high evaporative demand (Yokoyama et al., 2021). Consequently, leaf wetting increases the photosynthetic rate in the long term by mitigating water stress (Yokoyama et al., 2021). Leaf wetting is also linked with pathogen detection, thus continuous monitoring can help in the early detection of pathogens (Dawson & Goldsmith, 2018).

The ability of bioristor to detect leaf wetting is mainly due to the variation in solutes content in the plant sap due to environmental conditions. Changes in water potential lead to changes in the concentration of solutes (i.e. leaf osmolality), which then impact on the primary and secondary metabolism (Dawson & Goldsmith, 2018) as highlighted by the high correlation observed between R and VPD values (Figs. 4 and 7, Vurro et al., 2019).

A side result of this field trial was the determination of the half-life of the pesticides by continuous monitoring during the field trial. During the 2018 season, a strong change in the slope of the sensor response was associated with the use of an anti-aphid treatment (ACTARA 25WG). In fact, the mode of action of ACTARA in the plant was similar to the one triggered during severe drought stress, thus leading, in terms of sensor response, to a major change in the value and trend of the R index. The analysis of R also enabled the ACTARA half-life to be estimated as 13 days which to the best of our knowledge has not been reported before.

Conclusions

This study has demonstrated that bioristor enables real time, in vivo and continuous monitoring of tomato growth and fruit production in open field conditions, resulting in the identification of the sensor response index (R index), that has been demonstrated to be a good proxy of plant health status. Of note, bioristor allowed to trace the plant's water status dynamics during the plant response under changing environmental conditions together with the precise occurrence and duration of the drought stress. The use of bioristor for smart agriculture can concretely contribute to improve the sustainable use of water in agriculture leading to save 36–38% of the water consumed for irrigation.

A novel feature of bioristor was also identified. The frequency, timing, and duration of leaf wetting was also established through the analysis of the R index, leading to further optimization of water use, and opening new perspectives on pest detection, and management since a pathogen attack is strictly related to plant humidity. This bioristor's feature would enable a more precise schedule of pesticide treatment, thereby contributing to greater sustainability in agriculture.

Taking all together, this work paves the way for the use of bioristor under a smart irrigation approach significantly improves the water use efficiency allowing the fine-tuning of irrigation protocols and strategies.

Data availability The datasets generated during the current study are available from the corresponding author on reasonable request.

Declarations

References

Amato, D., Montanaro, G., Vurro, F., Coppedé, N., Briglia, N., Petrozza, A., Michela, J., Zappettini, A., Cellini, F., & Nuzzo, V. (2021). Towards in vivo monitoring of ions accumulation in trees: response of an in planta organic electrochemical transistor based sensor to water flux density, light and vapor pressure deficit variation. *Applied Sciences, 11*(11), 4729. https://doi.org/10.3390/app11114729

Balafoutis, A. T., Koundouras, S., Anastasiou, E., Fountas, S., & Arvanitis, K. (2017). Life cycle assessment of two vineyards after the application of precision viticulture techniques: a case study. *Sustainability, 9*(11), 1997. https://doi.org/10.3390/su9111997

Barrs, H., D., & Weatherley, P., E (1962). A re-examination of the relative turgidity technique for estimating water deficits in leaves. *Australian Journal of Biological Sciences*, *15*, 413–428.

Ben Hamed, K., Zorrig, W., & Hamzaoui, A. H. (2016). Electrical impedance spectroscopy: a tool to investigate the responses of one halophyte to different growth and stress conditions. *Computers and Electronics in Agriculture, 123*, 376–383. https://doi.org/10.1016/j.compag.2016.03.006

Ben Mariem, S., Soba, D., Zhou, B., Loladze, I., Morales, F., & Aranjuelo, I. (2021). Climate change, crop yields, and grain quality of C3 cereals: a meta-analysis of [CO_2], temperature, and drought effects. *Plants, 10*(6), 1052. https://doi.org/10.3390/plants10061052

Bernacka-Wojcik, I., Huerta, M., Tybrandt, K., Karady, M., Mulla, M. Y., Poxson, D. J., Gabrielsson, E. O., Ljung, K., Simon, D. T., Berggren, M., & Stavrinidou, E. (2019). Implantable organic electronic ion pump enables ABA hormone delivery for control of stomata in an intact tobacco plant. *Small (Weinheim An Der Bergstrasse, Germany), 15*(43), 1902189. https://doi.org/10.1002/smll.201902189

Bonfante, A., Monaco, E., Manna, P., & De Mascellis, R. (2019). LCIS DSS—an irrigation supporting system for water use efficiency improvement in precision agriculture: a maize case study. *Agricultural Systems*. https://doi.org/10.1016/j.agsy.2019.102646

Browne, M., Yardimci, N. T., Scoffoni, C., Jarrahi, M., & Sack, L. (2020). Prediction of leaf water potential and relative water content using terahertz radiation spectroscopy. *Plant Direct*, *4*(4), e00197. https://doi.org/10.1002/pld3.197.

Buffagni, V., Vurro, F., Janni, M., Gullì, M., Keller, A. A., & Marmiroli, N. (2020). Shaping durum wheat for the future: gene expression analyses and metabolites profiling support the contribution of BCAT genes to drought stress response. *Frontiers in Plant Science*. https://doi.org/10.3389/fpls.2020.00891

Cabrita, P. (2022). Non-invasive assessment of the physiological role of leaf aerenchyma in *Hippeastrum* herb. and its relation to plant water status. *Planta, 256*(1), 19. https://doi.org/10.1007/s00425-022-03930-2

Cantore, V., Lechkar, O., Karabulut, E., Sellami, M. H., Albrizio, R., Boari, F., Stellacci, A. M., & Todorovic, M. (2016). Combined effect of deficit irrigation and strobilurin application on yield, fruit quality and water use efficiency of "cherry" tomato (*Solanum lycopersicum* L.). *Agricultural Water Management, 167*, 53–61. https://doi.org/10.1016/j.agwat.2015.12.024

Coppedè, N., Janni, M., Bettelli, M., Maida, C. L., Gentile, F., Villani, M., Ruotolo, R., Iannotta, S., Marmiroli, N., Marmiroli, M., & Zappettini, A. (2017). An in vivo biosensing, biomimetic electrochemical transistor with applications in plant science and precision farming. *Scientific Reports, 7*(1), 16195. https://doi.org/10.1038/s41598-017-16217-4

Coppedè, N., Villani, M., & Gentile, F. (2014). Diffusion driven selectivity in organic electrochemical transistors. *Scientific Reports*. https://doi.org/10.1038/srep04297

Corbari, C., Ben Charfi, I., & Mancini, M. (2021). Optimizing irrigation water use efficiency for tomato and maize fields across italy combining remote sensing data and the aquacrop model. *Hydrology, 8*(1), 39. https://doi.org/10.3390/hydrology8010039

Dawson, T. E., & Goldsmith, G. R. (2018). The value of wet leaves. *New Phytologist*, *219*(4), 1156–1169. https://doi.org/10.1111/nph.15307.

Diacci, C., Abedi, T., Lee, J. W., Gabrielsson, E. O., Berggren, M., Simon, D. T., Niittyla, T., & Stavrinidou, E. (2021). Diurnal in vivo xylem sap glucose and sucrose monitoring using implantable organic electrochemical transistor sensors. *iScience*. https://doi.org/10.1016/j.isci.2020.101966

Dufil, G., Bernacka-Wojcik, I., Armada-Moreira, A., & Stavrinidou, E. (2022). Plant bioelectronics and biohybrids: the growing contribution of organic electronic and carbon-based materials. *Chemical Reviews, 122*(4), 4847–4883. https://doi.org/10.1021/acs.chemrev.1c00525

Ehrenberger, W., Rüger, S., Rodríguez-Domínguez, C. M., Díaz-Espejo, A., Fernández, J., Moreno, J., Zimmermann, D., Sukhorukov, V. L., & Zimmermann, U. (2012). Leaf patch clamp pressure probe measurements on olive leaves in a nearly turgorless state. *Plant Biology, 14*(4), 666–674. https://doi.org/10.1111/j.1438-8677.2011.00545.x

FAO (2021). The state of Food and Agriculture 2021. Making agrifood systems more resilient to shocks and stresses. Rome, FAO. https://doi.org/10.4060/cb1447en

Fariñas, M. D., Sancho-Knapik, D., Peguero-Pina, J. J., Gil-Pelegrín, E., & Gómez Álvarez-Arenas, T. E. (2022). Contact-less, non-resonant and high-frequency ultrasonic technique: towards a universal tool for plant leaf study. *Computers and Electronics in Agriculture, 199*, 107160. https://doi.org/10.1016/j.compag.2022.107160

Finco, A., Bentivoglio, D., Chiaraluce, G., Alberi, M., Chiarelli, E., Maino, A., Mantovani, F., Montuschi, M., Raptis, K. G. C., Semenza, F., Strati, V., Vurro, F., Marchetti, E., Bettelli, M., Janni, M., Anceschi, E., Sportolaro, C., & Bucci, G. (2022). Combining precision viticulture technologies and economic indices to sustainable water use management. *Water, 14*(9), 1493. https://doi.org/10.3390/w14091493

Fotia, K., Mehmeti, A., Tsirogiannis, I., Nanos, G., Mamolos, A. P., & Malamos, N. (2021). LCA-based environmental performance of olive cultivation in northwestern Greece: from rainfed to irrigated through conventional and smart crop management practices. *Water, 13*(14), 1954. https://doi.org/10.3390/w13141954

Friedlein, J. T., McLeod, R. R., & Rivnay, J. (2018). Device physics of organic electrochemical transistors. *Organic Electronics*, *63*, 398–414. https://doi.org/10.1016/j.orgel.2018.09.010.

Gebbers, R., & Adamchuk, V. I. (2010). Precision agriculture and food security. *Science, 327*(5967), 828–831. https://doi.org/10.1126/science.1183899

Gentile, F., Vurro, F., Picelli, F., Bettelli, M., Zappettini, A., & Coppedè, N. (2020). A mathematical model of OECTs with variable internal geometry. *Sensors and Actuators A: Physical*, *304*, 111894. https://doi.org/10.1016/j.sna.2020.111894.

Gu, Z., Qi, Z., Burghate, R., Yuan, S., Jiao, X., & Xu, J. (2020). Irrigation scheduling approaches and applications: a review. *Journal of Irrigation and Drainage Engineering, 146*(6), 04020007. https://doi.org/10.1061/(ASCE)IR.1943-4774.0001464

Jamaludin, D., Abd Aziz, S., Ahmad, D., & Jaafar, H. Z. E. (2015). Impedance analysis of *Labisia pumila* plant water status. *Information Processing in Agriculture, 2*(3), 161–168. https://doi.org/10.1016/j.inpa.2015.07.004

Janni, M., Claudia, C., Federico, B., Sara, P., Filippo, V., Nicola, C., Manuele, B., Davide, D., Loreto, F., & Zappettini, A. (2021). Real-time monitoring of arundo donax response to saline stress through the application of in vivo sensing technology. *Scientific Reports, 11*(1), 18598. https://doi.org/10.1038/s41598-021-97872-6

Janni, M., Coppede, N., Bettelli, M., Briglia, N., Petrozza, A., Summerer, S., Vurro, F., Danzi, D., Cellini, F., Marmiroli, N., Pignone, D., Iannotta, S., & Zappettini, A. (2019). In vivo phenotyping for the early detection of drought stress in tomato. *Plant Phenomics*. https://doi.org/10.34133/2019/6168209

Jiang, G. L. (2020). Comparison and application of non-destructive NIR evaluations of seed protein and oil content in soybean breeding. *Agronomy*, *10*(1), 77. https://doi.org/10.3390/agronomy10010077.

Jócsák, I., Végvári, G., & Vozáry, E. (2019). Electrical impedance measurement on plants: a review with some insights to other fields. *Theoretical and Experimental Plant Physiology, 31*(3), 359–375. https://doi.org/10.1007/s40626-019-00152-y

Kaiser, H., Sagervanshi, A., & Mühling, K. H. (2022). A method to experimentally clamp leaf water content to defined values to assess its effects on apoplastic pH. *Plant Methods*, *18*(1), 72. https://doi.org/10.1186/s13007-022-00905-y.

Kassambara, A., & Mundt, F. (2016) Factoextra: extract and visualize the results of multivariate data analyses. https://CRAN.R-project.org/package=factoextra r package version 1.0.3.

Kim, M. Y., & Lee, K. H. (2022). Electrochemical sensors for sustainable precision agriculture—a review. Frontiers in Chemistry, 10. Retrieved August 25, 2022 from https://www.frontiersin.org/articles/10.3389/fchem.2022.848320

Li, R., Lu, Y., Peters, J. M. R., Choat, B., & Lee, A. J. (2020). Non-invasive measurement of leaf water content and pressure–volume curves using terahertz radiation. *Scientific Reports*, *10*(1), 21028. https://doi.org/10.1038/s41598-020-78154-z.

Loures, L., Chamizo, A., Ferreira, P., Loures, A., Castanho, R., & Panagopoulos, T. (2020). Assessing the effectiveness of precision agriculture management systems in mediterranean small farms. *Sustainability, 12*(9), 3765. https://doi.org/10.3390/su12093765

Marquez, A. V., McEvoy, N., & Pakdel, A. (2020). Organic electrochemical transistors (OECTs) toward flexible and wearable bioelectronics. *Molecules, 25*(22), 5288. https://doi.org/10.3390/molecules25225288

Millones-Chanamé, C. E., de Oliveira, A. M. S., de Castro, E. M., & Maluf, W. R. (2019). Inheritance of blossom end rot resistance induced by drought stress and of associated stomatal densities in tomatoes. *Euphytica*, *215*(7), 120. https://doi.org/10.1007/s10681-019-2444-z.

Mundim, F. M., & Pringle, E. G. (2018). Whole-plant metabolic allocation under water stress. *Frontiers in Plant Science*. https://doi.org/10.3389/fpls.2018.00852

Parihar, G., Saha, S., & Giri, L. I. (2021). Application of infrared thermography for irrigation scheduling of horticulture plants. *Smart Agricultural Technology*, *1*, 100021. https://doi.org/10.1016/j.atech.2021.100021.

Polinova, M., Salinas, K., Bonfante, A., & Brook, A. (2019). Irrigation optimization under a limited water supply by the integration of modern approaches into traditional water management on the cotton fields. *Remote Sensing, 11*(18), 2127. https://doi.org/10.3390/rs11182127

Poxson, D. J., Karady, M., Gabrielsson, R., Alkattan, A. Y., Gustavsson, A., Doyle, S. M., Robert, S., Ljung, K., Grebe, M., Simon, D. T., & Berggren, M. (2017). Regulating plant physiology with organic electronics. *Proceedings of the National Academy of Sciences of the United States of America, 114*(18), 4597–4602. https://doi.org/10.1073/pnas.1617758114

Ritchie, H., & Roser, M. (2020). Environmental impacts of food production. *Our World in Data*. https://ourworldindata.org/environmental-impacts-of-food. Accessed 25 February 2021.

Sancho-Knapik, D., Peguero-Pina, J. J., Fariñas, M. D., Álvarez-Arenas, T. G., & Gil-Pelegrín, E. (2013). Ultrasonic spectroscopy allows a rapid determination of the relative water content at the turgor loss point: a comparison with pressure–volume curves in 13 woody species. *Tree Physiology, 33*(7), 695–700. https://doi.org/10.1093/treephys/tpt052

Shafi, U., Mumtaz, R., García-Nieto, J., Hassan, S. A., Zaidi, S. A. R., & Iqbal, N. (2019). Precision agriculture techniques and practices: from considerations to applications. *Sensors (Basel, Switzerland), 19*(17), 3796. https://doi.org/10.3390/s19173796

Stavrinidou, E. (2022). Bioelectronics for Plant Interface. In Stavrinidou, E. & Proctor, C. M. (Eds.), *Introduction to Bioelectronics* (pp: 12-1-12–22). AIP Publishing Books, AIP Publishing LLC. https://doi.org/10.1063/9780735424470_012

Stavrinidou, E., Gabrielsson, R., Gomez, E., Crispin, X., Nilsson, O., Simon, D. T., & Berggren, M. (2015). Electronic plants. *Science Advances*, *1*(10), e1501136. https://doi.org/10.1126/sciadv.1501136.

Stavrinidou, E., Gabrielsson, R., Nilsson, K. P. R., Singh, S. K., Franco-Gonzalez, J. F., Volkov, A. V., Jonsson, M. P., Grimoldi, A., Elgland, M., Zozoulenko, I. V., Simon, D. T., & Berggren, M. (2017). In vivo polymerization and manufacturing of wires and supercapacitors in plants. *Proceedings of the National Academy of Sciences of the United States of America, 114*(11), 2807–2812. https://doi.org/10.1073/pnas.1616456114

Takács, S., Pék, Z., Csányi, D., Daood, H. G., Szuvandzsiev, P., Palotás, G., & Helyes, L. (2020). Influence of water stress levels on the yield and lycopene content of tomato. *Water, 12*(8), 2165. https://doi.org/10.3390/w12082165

Tarabella, G., Villani, M., Calestani, D., Mosca, R., Iannotta, S., Zappettini, A., & Coppedè, N. (2012). A single cotton fiber organic electrochemical transistor for liquid electrolyte saline sensing. *Journal of Materials Chemistry*, *22*(45), 23830. https://doi.org/10.1039/c2jm34898e.

Vurro, F., Janni, M., Coppedè, N., Gentile, F., Manfredi, R., Bettelli, M., & Zappettini, A. (2019). Development of an in vivo sensor to monitor the effects of vapour pressure deficit (VPD) changes to improve water productivity in agriculture. *Sensors (Basel, Switzerland), 19*(21), 4667. https://doi.org/10.3390/s19214667

Wing, I. S., De Cian, E., & Mistry, M. N. (2021). Global vulnerability of crop yields to climate change. *Journal of Environmental Economics and Management*, *109*, 102462. https://doi.org/10.1016/j.jeem.2021.102462.

Wong, C. Y. S., Bambach, N. E., Alsina, M. M., McElrone, A. J., Jones, T., Buckley, T. N., Kustas, W. P., & Magney, T. S. (2022). Detecting short-term stress and recovery events in a vineyard using tower-based remote sensing of photochemical reflectance index (PRI). *Irrigation Science, 40*(4), 683–696. https://doi.org/10.1007/s00271-022-00777-z

Yin, H., Cao, Y., Marelli, B., Zeng, X., Mason, A. J., & Cao, C. (2021). Soil sensors and plant wearables for smart and precision agriculture. *Advanced Materials, 33*(20), 2007764. https://doi.org/10.1002/adma.202007764

Yokoyama, G., Yasutake, D., Minami, K., Kimura, K., Marui, A., Yueru, W., Feng, J., Wang, W., Mori, M., & Kitano, M. (2021). Evaluation of the physiological significance of leaf wetting by dew as a supplemental water resource in semi-arid crop production. *Agricultural Water Management, 255*, 106964. https://doi.org/10.1016/j.agwat.2021.106964

Zhang, Q., Li, Q., & Zhang, G. (2012). Rapid determination of leaf water content using VIS/NIR spectroscopy analysis with wavelength selection. *Journal of Spectroscopy, 27*, 93–105. https://doi.org/10.1155/2012/276795